

ASSESSING THE EFFECT OF PREDICTED CLIMATE CHANGE ON SLOPE STABILITY IN NORTHERN THAILAND: A CASE OF DOI PUI

* Thapthai Chaithong¹, Suttisak Soralump², Damrong Pungsuwan³, and Daisuke Komori⁴

^{1,4} Graduate of School of Environmental Studies, Tohoku University, Japan;

^{1,2,3} Geotechnical Engineering Research and Development Center, Department of Civil Engineering, Faculty of Engineering, Kasetsart University, Thailand

*Corresponding Author, Received: 2 Jan. 2017, Revised: 30 Jan. 2017, Accepted: 29 March 2017

ABSTRACT: Landslide is a natural disaster which occurs very often in mountainous areas. Climate is an important determinant on the amount of moisture in the ground, which is a key to the stability of soil slope. Therefore, climate change due to the global warming may affect the intensity of rainfall and the evaporation in the future and influences situation of slope stability in a long time. The purpose of this study is to propose a method for assessing the effect of climate change on slope stability using general circulation model (GCM). A method for predicting climate change impact on slope stability is to link the antecedent precipitation index (API), hydrological model, obtained through downscaling GCM to critical antecedent precipitation model. The GCM is downscaled using a dynamical technique to derive regional climate models. Then a statistical correlation is used to adjust for the basis of the regional climate model. The GCM used in this study is the ECHAM4/OPYC3 model. The analysis found that the trend of susceptibility to slope failure depends on the pattern of simulated rainfall and the recession constant of the antecedent precipitation index.

Keywords: Climate Change, Slope Stability, Antecedent Precipitation, General Circulation model, Unsaturated Soil behavior

1. INTRODUCTION

Thailand has been experiencing the effects of climate change. The Thai Meteorological Department reported that the annual mean maximum temperature in Thailand rose by approximately 0.75 degrees Celsius; in addition, the annual mean minimum temperature in Thailand rose by approximately 1 degree Celsius from 1951 to 2012. Reference [20] proposed that the number of rainy days has reduced remarkably, and the proportion of total rainfall from extreme rainfall has risen significantly at Nan province in the northern Thailand. The Intergovernmental Panel on Climate Change (IPCC) warns that the mean temperature of Southeast Asia region could rise by 4.8 degree Celsius by 2100 from 1990 levels.

Landslide, as one of the natural hazards, causes infrastructure damage, property damage, many deaths, and severe injuries. In many cases of landslide or slope failure, extreme or prolonged rainfall is the main trigger of the slope instability, such as, in 2006, landslides and flash floods triggered by heavy rain which the cumulative rainfall on 20-23 may 2006 was about 405 mm. The event affected five provinces in the northern part of Thailand. The influence of rainfall on the slope stability is very well understood. Rainwater seeps into the soil slope and generates the pore-water pressure or groundwater table. The

groundwater table and the pore-water pressure reduced effective stress and matric suction, and it affects the shear strength on the failure plane decrease. It leads to landslides or slope failures. In contrast, numerous researchers proposed the influence of evaporation that it may increase the slope stability [7], [16], [23]. The evaporation reduces soil moisture and pore-water pressure and increases the matric suction and effective stress. It has a positive influence on the shear strength of the slope and it leads to stabilize of the slope. Climate controls rainfall, evaporation, wind speed and the other. Hence, the climate is a significant factor in overall the soil slope stability. Therefore, the long-term climate model is very important for predicting the slope stability. The general circulation models (GCMs) are a possible attempt for estimating the future climate caused by the greenhouse gas. Numerous researchers used the GCMs and a landslide model for assessing the impact of climate change on the stability of slope [2]–[5], [8]–[12], [17]. Reference [12] analyzed the landslide activity change due to climate change, it was found that the return period of slope instability reduced in all the climate change scenarios because the higher temperature will tend to increase evapotranspiration and reduced effective precipitation. Reference [17] assess the climate change effect on landslides in the Canada, it was found that the total number of debris flows

may increase by approximately 30% by the end of the century and landslide frequency will increase during the twenty-first century along the southwest coast of British Columbia Canada. Reference [2] assessed the three landslides model for finding the most suitable landslide model for the effect of climate change on landslides in southeast France, it was found that the fully empirical climatic threshold (as a historical-critical rainfall threshold without considering the physical condition link), and, a semi-empirical climatic threshold (as a simple water balance model of the root zone with field observation data) were poorly correlated to historical case, in addition, conceptual slope model (as a combination between a hydrological and a slope stability model) was a potentially useful model but the uncertainty of parameter is a significant factor.

When considering the changing of rising temperature and variation rainfall, so the projection of climate in long-term condition is important for analysis situation of the slope stability. Hence, the aim of this study proposed a method of assessment situation of the slope stability, which combines the climate scenario and the critical rainfall threshold. The proposed method can find the critical rainfall threshold based on the soil moisture model and soil slope stability model.

2. DESCRIPTION OF STUDIED AREA

The studied site is a weathered granite rock slope in Songsaen Park, the Doi Pui research station of Kasetsart University, Chiang Mai province, Northern Thailand, as shown in Fig.1. The position is approximately 2079845.83N and 487848.14E, in addition, above mean sea level 1,250 meters. Geological condition of a studied site is the granite Triassic group, such as Biotite granite, Tourmaline granite, Muscovite – Tourmaline granite, and other. Ground profile at the site was investigated by borehole drilling methods and in-situ testing was standard penetration test (SPT). Undisturbed soil samples were performed by the test pit that it was excavated to a depth of 0.6 m for collection undisturbed soil samples. The soil strata consisted of 1.75-m-thick decomposed granite rock overlain by 1.25-m-thick silty sand and the top layer is 2.25-m-thick silty fines and sand with clayey fines (SM-SC). Fig.2 shows the soil profile and SPT value. Table 1 summarizes physical properties of the two materials at the site. The slope gradient at the site is 35 degrees.

The climate of this site is tropical wet and dry climate that is high relative humidity of air and a large amount of precipitation. Rainfall is about 1800 mm per year and the average temperature is

approximately 20 degree Celsius. Average relative humidity is between 56.7 % and 89.3 %. In addition, average wind speed is 7.7 km/hr. Fig. 3 shows the average monthly rainfall between 1966 and 1985 and monthly rainfall in 2015.

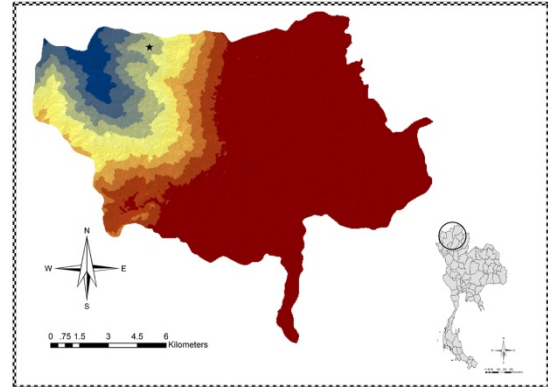


Fig.1 Location of the studied site

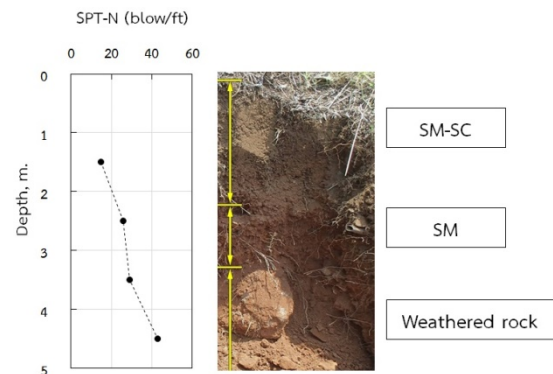


Fig.2 Soil profile and SPT value

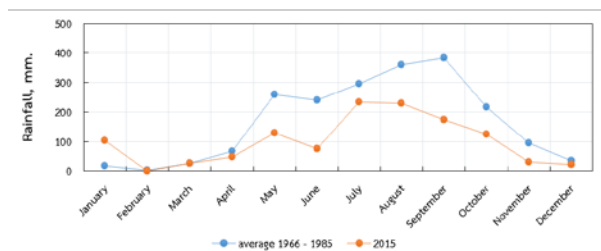


Fig.3 Average monthly rainfall during 1966 – 1985 and monthly rainfall 2015

Table 1 Physical soil properties

Description	SM-SC	SM
Natural water content (%)	11.1	10.8
Plasticity index (%)	5.5	NP
Void ratio	1.519	0.776
Dry density of soil, (kPa)	11.77	14.72

3. METHODOLOGY TO ASSESS THE EFFECT OF CLIMATE CHANGE ON SLOPE STABILITY

The proposed methodology is based on antecedent precipitation index model (API) as a result of general circulation model (GCM) and rainfall threshold model. Climate change scenario of GCM is used to calculate the antecedent precipitation index model which it is a slope hydrology model. The volume relationship of soil and infinite slope stability model are used to develop the rainfall threshold model, as known as a critical antecedent precipitation mode (CAPI). The simulation impact of climate change on the slope stability considers the following periods: 1. 1961-1990 (1970s, base period), 2. 2010-2039 (2020s, first future period), 3. 2040-2069 (2050s, second future period) and 4. 2070-2099 (2080s, third future period). Fig.4 depicts the methodology of linkage the GCMs and rainfall threshold model.

3.1 Predicted Climate Scenario

GCMs are the climate model that represents general circulation the process of the atmosphere and ocean based on a principal of thermodynamics, geophysical fluid dynamics, radiation transfer and the other processes. The GCMs are used to predict

the future climates have to couple the ocean general circulation models (OGCMS) and the atmospheric general circulation models (AGCMs). The AGCMs compute the process of winds, heat transfer, solar radiation, relative humidity, and surface hydrology in each grid and evaluate interactions with neighboring grids or points. The OGCMs calculate the evolution of ocean in horizontal and vertical velocity, ocean temperature, and salinity globally over the full depth of the ocean. The GCMs depict the earth's climate system using three-dimensional grids. The GCMs are typically having the horizontal resolution of between 250 and 600 km, moreover, 10 to 30 vertical layers. GCMs successfully simulate the climate scenarios in large-scale and long-term condition. Considering the horizontal resolution of GCMs, it was found that the horizontal resolution is very coarse (100 - 300 kilometers). It is a limitation and unsuitable for the regional area application. Hence, the downscaling approach is a solution of this limitation. The downscaling techniques have two main approaches: dynamical and statistical downscaling techniques. The climate model, as an output of the downscaling process, is can be called the regional climate model (RCM). [1]–[4], [8], [17]

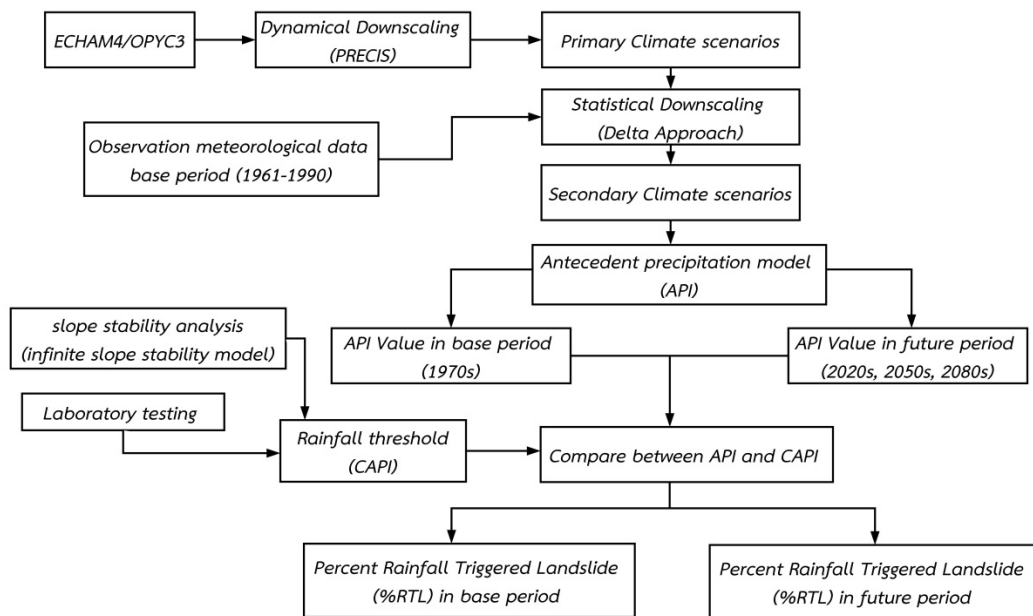


Fig.4 Methodology of linkage the GCMs and rainfall threshold model

This study uses ECHAM4/OPYC3 for predicting climate scenario. The ECHAM4/OPYC3 is the general circulation model which was developed by the Max - Planck institute for meteorological. The ECHAM4 is the atmospheric general circulation model and the

OPYC3 is the ocean general circulation model. The CO2 concentration has been estimated based on an IS92a scenario which follows the IPCC Second Assessment Report. The horizontal resolution of ECHAM4/OPYC3 is about 2.8×2.8 degrees ($\sim 300 \times 300$ km). The ECHAM4/PC3

passed the testing of a stable in a multi - century in second Couple Model Intercomparison Project of IPCC. This research used emission scenario B2 following the recommendation of the National Research Council of Thailand. Southeast Asia START Regional Center (START) provided data on the future climate projection, which is the high horizontal resolution. START used PRECIS (Providing REgional Climates for Impacts Studies) for creation the finer horizontal resolution. PRECIS is a regional climate modeling system based on the dynamical downscaling technique which is developed by the Met Office Hadley Centre. In this study, the future climate projection data of START is called a primary climate scenario. Regarding the difference between the RCM data and meteorological observation data, it was found that the RCM data will be prone to bias in the future climate data. Hence, this study applies the statistical approach to adjusting the bias. The output of bias adjustment is called a secondary climate scenario. Equation (1) shows an equation for precipitation and wind speed and Eq. (2) shows an equation for maximum and minimum temperature and relative humidity.

$$x_{new} = x_{obs,base} * \left(\frac{x_{RCM, future}}{x_{RCM, base}} \right) \quad (1)$$

$$x_{new} = x_{obs,base} + \left(\frac{x_{RCM, future} - x_{RCM, base}}{x_{RCM, base}} \right) \quad (2)$$

where x_{new} is scenarios climate parameters after correction bias, $x_{obs,base}$ is observed climate parameters in base period, $\frac{x_{RCM, future}}{x_{RCM, base}}$ is RCM climate parameters in future period, and $\frac{x_{RCM, future} - x_{RCM, base}}{x_{RCM, base}}$ is RCM climate parameters in base period.

In consideration of the observed weather data for adjustment bias of the RCM is based on the Thiessen polygon of weather station in northern Thailand. The study area is under the zone of Chiang Mai weather station. Therefore, the meteorological data from Chiang Mai weather station (station code, 48327) during 1961 to 1990 are chosen to adjust the bias of primary climate scenario. The meteorological data from 2010 to 2014 is selected to validate the reliability of secondary climate model; moreover, this research used root mean square error (RMSE) for comparison results of before and after adjustment as shown in Eq. (3). The meteorological data are checked and examined a consistency of data from double mass curve analysis. Examination results were found that the plot of double mass curve analysis is the straight line; hence, it means that the meteorological data have the consistency of

data record. Fig. 5 shows the Thiessen polygon of weather station in the northern Thailand. Fig. 6 shows the double mass curve of rainfall in Chiang Mai weather station.

$$RMSE = \sqrt{\frac{1}{n} \sum (x_{obs} - x_{scm})^2} \quad (3)$$

where RMSE is root mean square error, n is number of day, x_{obs} is observed climate data, and x_{scm} is secondary climate scenarios.

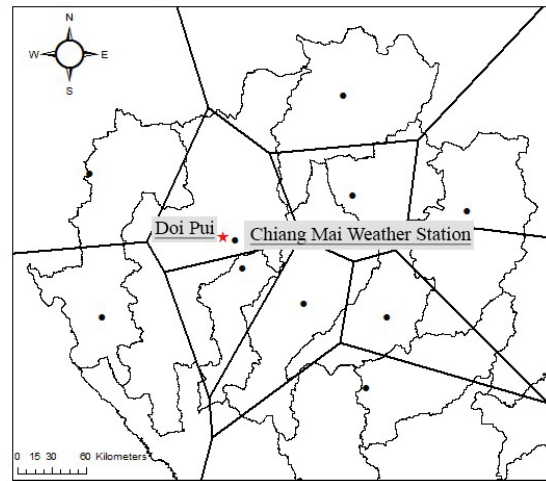


Fig.5 Thiessen polygon of weather station in the northern Thailand.

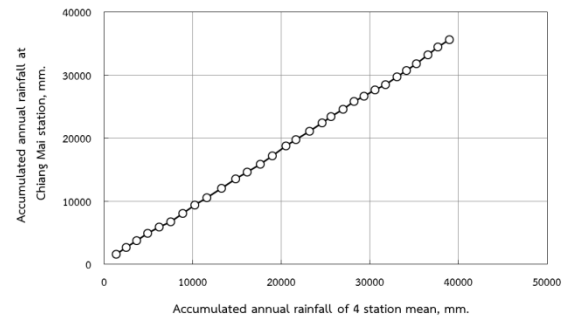


Fig.6 Double mass curve of rainfall for Chiang Mai weather station.

3.2 Antecedent precipitation index (API)

The antecedent rainfall plays a significant role in a situation of the soil slope. Reference [22] proposed that the antecedent rainfall during the five-day was significant in causing landslide. Reference [26] proposed the landslide warning criteria for northern Thailand, which used relationship the three-day antecedent rainfall and the rainfall in a day. Therefore, the hydrology model for this study is the antecedent precipitation index (API). The antecedent precipitation index is

an index of moisture stored within a soil mass which considers the previous and present rainfall.

API can use Eq. 4 for calculation. [24], [28], [29]

$$API_{(t)} = API_{(t-1)}K_{(t)} + P_{(t)} \quad (4)$$

where $API_{(t)}$ is API on day 't' (mm), $API_{(t-1)}$ is API on day 't-1', $K_{(t-1)}$ is a recession constant, and $P_{(t)}$ is precipitation on day 't'.

The equation to calculate the recession constant ($K_{(t-1)}$) shows in Eq. (5).

$$K_t = \exp(-E_t / W_m) \quad (5)$$

where E_t is the evaporation on day 't' and W_m is the maximum soil available for evaporation based on the function of soil water holding capacity (WHC), bulk density of soil (BD), and 100 mm is the soil depth as illustrated in Eq. (6).

$$W_m = (WHC / 100) \cdot BD \cdot 100(mm) \quad (6)$$

In 2015, reference [6] proposed the curves of the recession constant in each month during 2010 to 2099 which consider the evaporation change due to climate change using ECHAM4/OYPC3. Fig.7 shows the recession constant between 2010 and 2099. Therefore, this study used the recession constant which it was proposed.

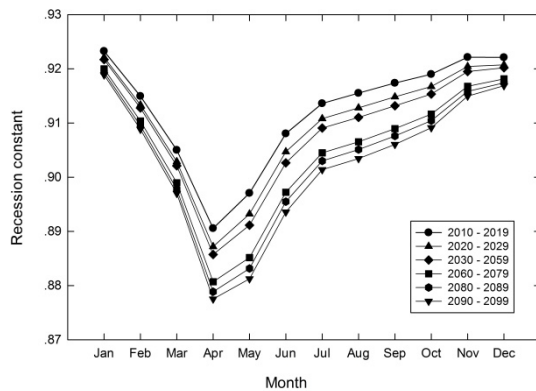


Fig.7 The recession constant between 2010 and 2099 [6]

3.3 Critical antecedent precipitation index

The critical antecedent precipitation index (CAPI) is an index of water absorbed in the void of soil mass when the safety factor of the soil slope equal to 1. The CAPI combines an indicator of the degree of saturation and the shearing resistance of soil slope. The CAPI value is calculated and used

as a susceptibility landslide analysis and a warning criterion for the landslide-prone area [19], [24], [28], [29]. There are three main parameters for CAPI calculation which include; the porosity, the critical degree of saturation, and the critical thickness of soil, as follows:

$$CAPI = \eta \cdot S_{r,cr} \cdot T_{cr} \quad (7)$$

where $S_{r,cr}$ is the critical degree of saturation, T_{cr} is the critical thickness of soil, and η is the porosity.

The critical thickness of soil concept is based on the infinite slope analysis model and the concept of extended Mohr-Coulumb failure criteria for unsaturated shear strength. The extended Mohr-Coulumb failure criterion is as follows [13]:

$$\tau = c' + (\sigma_n - u_a) \tan \phi' + (u_a - u_w) \tan \phi^b \quad (8)$$

where τ is the shear strength of the unsaturated soil, c' is the effective cohesion, ϕ' is the effective angle of internal friction, $(\sigma_n - u_a)$ is the effective normal stress on the plane of failure, $(u_a - u_w)$ is the matric suction on the plane of failure, and ϕ^b is angle indicating the rate of increase of shear strength relative to increase matric suction.

The concept of stability of hillslope is presented in the form of factor of safety, which is the ratio of shear strength to shear stress. If the factor of safety becomes less than 1.0, the hill slope is instability. The infinite slope analysis model used to calculate the critical thickness of soil because the characteristics of the landslide are shallow depth (1-2 meter) and along a failure plane parallel to a ground surface, so, agree with the mode of failure of the infinite slope model. The factor of safety (FS) equation is as follows:

$$FS = \frac{c' + (\sigma_n - u_a) \tan \phi' + (u_a - u_w) \tan \phi^b}{\gamma T \cos \beta \sin \beta} \quad (9)$$

where τ is the shear strength of the unsaturated soil, c' is the effective cohesion, ϕ' is the effective angle of internal friction, $(\sigma_n - u_a)$ is the effective normal stress on the plane of failure, $(u_a - u_w)$ is the matric suction on the plane of failure, ϕ^b is angle indicating the rate of increase of shear strength relative to increase matric suction, γ is the unit weight of the soil, T is the thickness of the soil slope, and β is the slope angle.

The critical thickness, T_{cr} is the soil depth when a soil slope starts to be unstable ($FS = 1$), and derived from Eq. (9). The critical thickness is as follows:

$$T_{cr} = \frac{c' + (\sigma_n - u_a) \tan \phi' + (u_a - u_w) \tan \phi^b}{\gamma \cos \beta \sin \beta} \quad (10)$$

From Eq. (7) and Eq. (10), CAPI can be calculated thus:

$$CAPI = \eta \cdot S_{r,cr} \left(\frac{c' + (\sigma_n - u_a) \tan \phi' + (u_a - u_w) \tan \phi^b}{\gamma \cos \beta \sin \beta} \right) \quad (11)$$

3.4 Percent rainfall triggered landslides

Reference [26] proposed the percent rainfall triggered landslides (RTL) for analysis a relationship between the antecedent precipitation index and the critical antecedent precipitation index that is an indicator of soil slope failure susceptibility. RTL is the ratio between the antecedent precipitation index and the critical antecedent precipitation index as shown in Eq. (12). Table 2 presents an index of the percent rainfall triggered landslides.

$$RTL = API_t / CAPI \quad (12)$$

Table 2 Index of the percent rainfall triggered landslides [25]

RTL, %	FS	Definition of landslides susceptibility
> 55	< 1.1	Very high
55 – 35	1.1 – 1.3	High
35 – 20	1.3 – 1.5	Medium
< 20	> 1.5	Low

Table 3 Multi-stage shear testing program

Specimen No.	Matric suction, kPa	Stage 1, Normal stress, kPa	Stage 2, Normal stress, kPa	Stage 3, Normal stress, kPa
1	0.1	32	64	128
2	1.5	32	64	128
3	51	32	64	128

5. RESULTS AND DISCUSSION

5.1 Predicted climate scenario

The performance of ECHAM4/OYPC3 for future climate scenarios was verified by using historical climate data for 2010-2014. Table 4 shows the RMSE before and after adjustment the primary climate model biases. According to the adjustment, it was found that the statistical

4. LABORATORY TESTS

Shear strength characteristic of the soil at the studied slope was investigated by the direct shear test under saturated and unsaturated condition. The undisturbed soil samples collected using the KU-Miniature sampler. This study applied a multi-stage shear test for finding shear strength parameters of the undisturbed soil sample. The multi-stage shear test is not an ASTM standard, but numerous researchers applied this technique for shearing the soil sample [14], [15], [18], [21], [26]. The benefits of the multi-stage technique are: 1 the effect of soil sample variability was completely removed and 2 usages the soil sample is less than the single-stage technique which is suitable for a difficult to access place. In this study, there are three different the matric suction and normal stress. To maintain constant moisture content during shearing, a plastic wrapping and wet clothes were used to cover the shear box. For this propose, the specimen no. 1 is the saturated condition which has a degree of saturation about 96.65%. The shearing rate is 0.01 mm/min because it is slowly enough to prevent the development of significant pore water pressures during shearing. The most important requirement of the multi-stage shear test is that the loading in each stage should not exceed the peak shear stress. The applied normal stresses and matric suction used in the multi-stage shear test are presented in Table 3. Fig. 8 presents typical results from multi-stage direct shear on a specimen No. 3. The net normal stress was increased from 32 to 128 kPa in 3 shearing stages. Fig. 9 presents a Mohr-Coulomb the failure envelopes obtained from multi-stage direct shear tests. Fig. 10 presents an unsaturated failure envelopes obtained from multi-stage direct shear test.

approach can increase the performance of predicted climate scenario because all of RMSE after adjustment in each climate parameter is decreased. The reduction of RMSE before and after adjustment is about 7.5% of rainfall, about 15% of maximum temperature, about 37.7% for minimum temperature, about 35.3% for wind speed, and 88% for relative humidity. Fig. 11 compares the monthly rainfall for 2010-2014 from Chiang Mai weather station and before-after biases correction. The figure shows, after bias correction,

the predicted rainfall better matches the observations from Chiang Mai weather station.

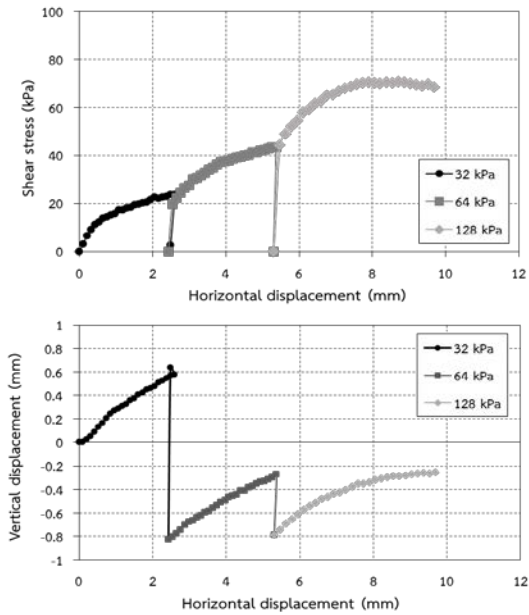


Fig.8 Results of multi-stage direct shear test for specimen No. 3.

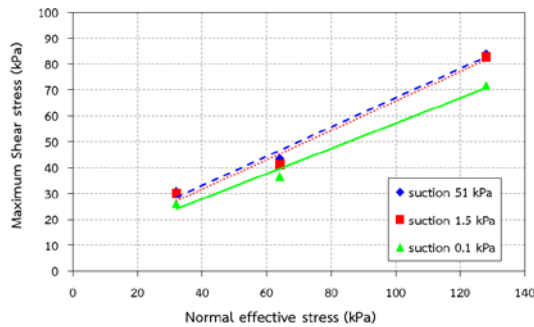


Fig.9 Mohr-Coulomb the failure envelopes obtained from multi-stages direct shear tests

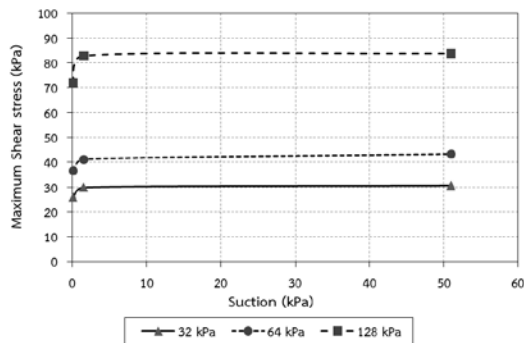


Fig.10 Unsaturated failure envelopes obtained from multi-stage direct shear tests.

Table 4 RMSE before and after adjustment the primary climate model biases

Parameter	Rainfall	
	RMSE	Accuracy, %
Before	1.18	7.48
After	1.09	
Parameter	Maximum Temperature	
	RMSE	Accuracy, %
Before	4.47	14.93
After	3.80	
Parameter	Minimum Temperature	
	RMSE	Accuracy, %
Before	3.93	37.74
After	2.44	
Parameter	Wind speed	
	RMSE	Accuracy, %
Before	4.90	35.33
After	3.17	
Parameter	Relative humidity	
	RMSE	Accuracy, %
Before	1048.43	87.89
After	126.92	

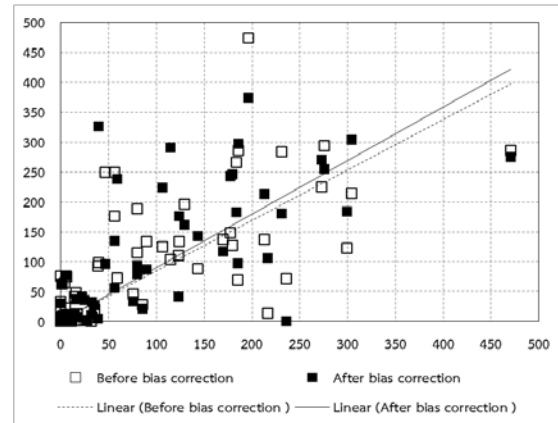


Fig.11 Monthly rainfall for 2010-2014 from Chiang Mai weather station and before-after biases correction.

The future prediction of the rainfall has been obtained from the secondary climate scenario using the B2 emission scenario of ECHAM4/OPYC3. The simulated future rainfalls of the 30-year time interval from 2010 to 2099 are summarized in table 5. Regarding the trend of projection rainfall, it was found that the average rainfall in the 2020s, 2050s, and 2080s does not significantly change in comparison the base period (1970s). Fig. 12 compares monthly simulated rainfalls in the 1970s, 2020s, 2050s, 2080s and historical observation rainfall at Doi Pui. Considering the difference rainfall between observation and simulation rainfall in 2015 at Doi

Pui, it was found that the simulated rainfall is more than the observed rainfall about 23.87%, and, the average simulated rainfall during 1966-1985 is less than the average observation rainfall about 23.3%. In addition, there is the significant difference between historical observation and simulated rainfall in May. However, the simulated future rainfall can present the behavior of rainfall in the monsoon season during mid-May – October. Fig. 13 compares mean monthly simulated maximum temperature in future period and historical observation data in 1966-1985 at Doi Pui. The mean monthly maximum temperature is predicted to rise about 3.2% for the 2020s, 19.1% for 2050s, and 22.5% for 2080s. Moreover, the mean annual maximum temperature rises about 2.6 degree Celsius at the end of the century. Fig. 14 compares mean monthly simulated minimum temperature in future period and historical observation data in 1966-1985 at Doi Pui. The mean monthly minimum temperature is predicted to rise about 5.8 degree Celsius at the end of century, and, an increase of 20% for the 2020s, 30% for 2050s, and 61% for 2080s.

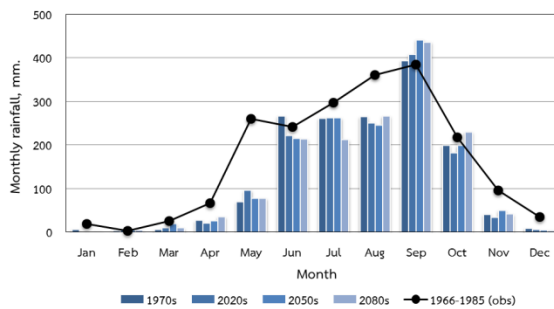


Fig.12 Monthly simulated rainfalls in the 1970s, 2020s, 2050s, 2080s and historical observation rainfall at Doi Pui

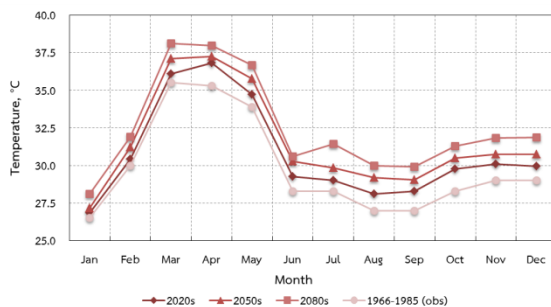


Fig.13 Mean monthly simulated maximum temperature in future period and historical observation data in 1966-1985 at Doi Pui

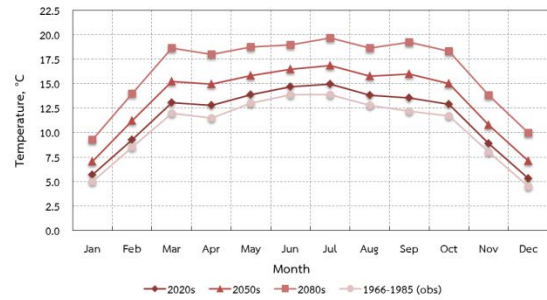


Fig.14 Mean monthly simulated minimum temperature in future period and historical observation data in 1966-1985 at Doi Pui.

Table 5 Simulated future rainfalls of the 30-year time interval from 2010 to 2099

Interval year	2020s	2050s	2080s
Rainfall, mm.	1,500.53	1,546.34	1,532.01

5.2 Simulated future landslide susceptibility

The CAPI calculation is using an Eq. (10), parameters as shown in table 1, and figure 5 and 6. According to the calculation, it showed that the CAPI value of the studied site is 814.05 mm. For this study, the degree of saturation used the CAPI calculation of study slope used 90% because this value was recommended by reference 29 that was suitable to calculate the CAPI for the weathered granite Triassic rock slope. Fig. 15 shows the expected antecedent precipitation index between 2010 and 2099. The peak of the expected antecedent precipitation index occurs in 2010, 2016, 2036, 2040, 2046, 2066, 2070, 2076, and 2096 which the API of each year is over 250 mm. Return period of the peak API is 10 years. Table 5 presents the percent rainfall triggered landslide (RTL) in the 1970s, 2020s, 2050s, and 2080s. When comparison the RTL between the base period (1970s) and the future periods (2020s, 2050s, and 2080s), it was found that the RTL of the future periods has increased for low landslide susceptibility (RTL < 20%). For the RTL < 20%, the trend decline about 0.03% during the 2020s - 2050s and rising about 0.3% in the third future period (2080s). The trend of medium susceptibility to slope failure (RTL 20%– 35%) is an increase of 3% from the 2020s to 2050s and a decrease about 28% in the third future period (2080s). Moreover, the trend remains steady over the 2020s and the 2050s and decline about 50% in the 2080s for the high susceptibility to slope failure (RTL 35% - 55%). The results of calculation showed that there was no value in excess of very high landslide susceptibility (RTL >55%). Fig. 16 shows the

number of exceedence days derived from comparison between base and three future periods. First, comparison between the base periods (1970s) and the first future periods (2020s), it was found that the number of days is an increase of 22 days for low landslide susceptibility (RTL < 20%), and a decrease of 21 days for medium landslide susceptibility (RTL 20%– 35%), in addition, a decrease of 1 day for high susceptibility to slope failure (RTL 35% - 55%). Next, considering to difference between the base periods (1970s) and the second future periods (2050s), it was found that the number of days is an increase of 19 days

for low landslide susceptibility (RTL < 20%), and a decrease of 18 days for medium landslide susceptibility (RTL 20%– 35%), in addition, a decrease of 1 day for high landslide susceptibility (RTL 35% - 55%). Last, regarding to the difference between the base periods (1970s) and the third future periods (2080s), it was found that the number of days is an increase of 51 days for low landslide susceptibility (RTL < 20%), and a decrease of 48 days for landslide susceptibility (RTL 20%– 35%), in addition, a decrease of 3 days for high landslide susceptibility (RTL 35% - 55%).

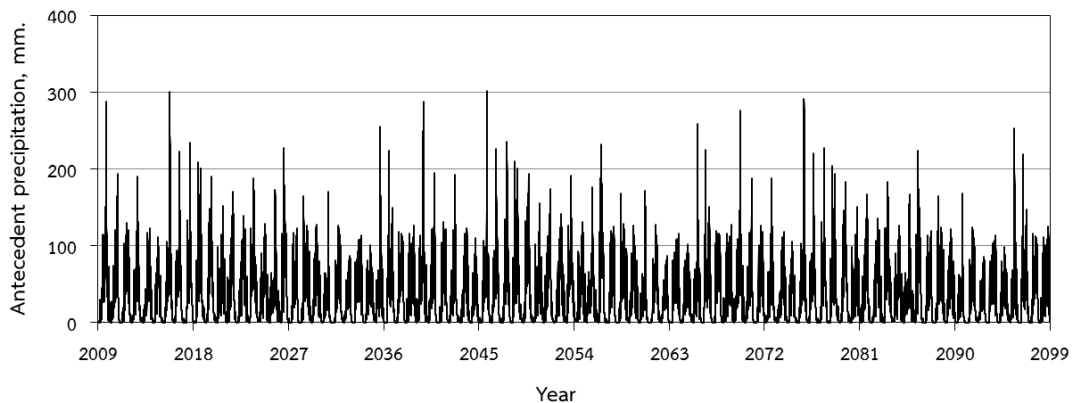


Fig. 15 Expected antecedent precipitation index between 2010 and 2099.

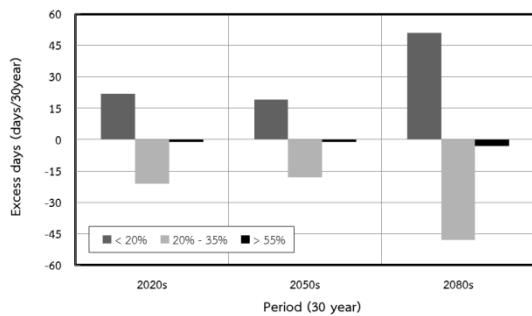


Fig. 16 Number of exceedence days derived from comparison between base and three future periods

Therefore, when considering factors affecting the trend of susceptibility to landslides, it was found that the decrease in future simulated rainfall affects susceptibility of landslide occurrence. In the future periods, the trend of susceptibility to landslides is an increase between the 2020s and 2050s but a decrease in the 2080s because the predicted rainfall is an increase of about 3% during the 2020s to 2050s but a decrease of about 1%. Moreover, the effect of recession constant is significant on the susceptibility to landslides because of the recession constant declines over

time. Therefore, the reduction of susceptibility to landslides in the third future year receives the influence of the recession constant decreasing. Reference [6] proposed that the increase with time in evaporation based on computation affect the recession constant decrease with time. Hence, the increase in evaporation will have an influence on the susceptibility of landslide occurrence in the future.

6. CONCLUSIONS

Assessing the effect of future climate using the ECHAM4/OYPC3 and the CAPI on the slope stability, it could be concluded; the pattern of rainfall play important role in the trend of slope failure occurrence in the future, in addition, the recession constant of API changing due to evaporation changing is control the pattern of antecedent rainfall that it changes over time. The large difference between the simulated and observed rainfall is the weakest point of analysis because the secondary climate scenario needs to use the correlation between the simulated and observed data.

7. ACKNOWLEDGEMENTS

The authors would like to acknowledge the Southeast Asia START Regional Center for providing the regional climate model and also the Thai meteorological department (TMD) for patronage the meteorological observation data, and gratefully thank you department of mineral resource (DMR), department of water resource (DWR) and Geotechnical Engineering Research and Development Center (GERD) for support field and site investigation. The authors would sincerely like to thank Assoc. Prof. Dr. Apiniti Jotisankasa for equipment and suggestion and the Doi Pui research station of Kasetsart University for place and the other. A special thank you, Asst. Prof. Dr. Jirawat Ganasut for the good recommendation about GCMs.

8. REFERENCES

- [1] Amin, M. Z. M., Islam, T., & Ishak, A. M. Downscaling and Projection of Precipitation from General Circulation Model Predictors in an Equatorial Climate Region by the Automated Regression-based Statistical Method. *Theoretical and Applied Climatology*, Vol. 118, 2014, pp. 347-364.
- [2] Buma, J. Finding the Most Suitable Slope Stability Model for the Assessment of the Impact of Climate Change on A Landslide in Southeast France. *Earth Surface Processes and Landforms*, Vol. 25, 2000, pp. 565-582.
- [3] Buma, J., & Dehn, M. A Method for Predicting the Impact of Climate Change on Slope Stability. *Environmental Geology*, Vol. 35, 1998, pp. 190-196.
- [4] Buma, J., & Dehn, M. Impact of Climate Change on a Landslide in South East France Simulated Using Different GCM Scenarios and Downscaling Methods for Local Precipitation. *CLIMATE RESEARCH*, Vol. 15, 2000, pp. 69-81.
- [5] Buma, J., & Dehn, M. Modelling Future Landslide Activity Based on General Circulation Models. *Geomorphology*, Vol. 30, 1990, pp. 175-187.
- [6] Chaithong, T. Investigation of Evaporation Effect on Slope Stability in Relation to Climate Change. Master Thesis, Kasetsart University, Thailand, 2015.
- [7] Chaithong, T., & Soralump, S. The Effect of Evaporation Flux Boundary Condition on Pore Water Pressure in Hillslope. *Proceedings the 20th National Convention on Civil Engineering*, Thailand, 2015.
- [8] Chiang, T., & Chang, K. T. The Potential Impact of Climate Change on Typhoon-triggered Landslides in Taiwan 2010-2009. *Geomorphology*, Vol. 133, 2011, pp. 143-151.
- [9] Collison, A., Wade, S., Griffiths, J., & Dehn, M. Modelling the Impact of Predicted Climate Change on Landslide Frequency and Magnitude in SE England. *Engineering Geology*, Vol. 55, 2000, pp. 205-218.
- [10] Damiano, E., & Mercogliano, P. Potential Effects of Climate Change on Slope Stability in Unsaturated Pyroclastic Soils. *Landslide Science and Practice*, Vol. 4, 2013, pp. 15-25.
- [11] Dehn, M., Burger, G., Buma, J., & Gasparetto, P. Impact of Climate Change on Slope Stability using Expanded Downscaling. *Engineering Geology*, Vol. 55, 2000, pp. 193-204.
- [12] Dixon, N., & Brook, E. Impact of Predicted Climate Change on Landslide Reactivation: Case Study of Mam Tor, UK. *Landslides*, Vol. 4, 2007, pp. 137-147.
- [13] Fredlund, D. G., Rahardjo, H., & Gan, K. J. Seismic Stability and Permanent Deformation Analyses: The Last Twenty-five Years. *Proceeding 6th International Conference on Expansive Soils*, India, 1987, pp. 49-54.
- [14] Gan, K. J., & Fredlund, D. G. Multistage Direct Shear Testing of Unsaturated Soils. *Geotechnical Testing Journal*, Vol. 11, No. 2, 1988, pp. 132-138.
- [15] Gan, K. J., & Fredlund, D. G. Shear Strength Characteristics of Two Saprolitic Soils. *Canadian Geotechnical Journal*, Vol. 33, 1996 pp. 595-609.
- [16] Gasmo, J. M., Rahardjo, H., & Leong, E. C. Infiltration Effects on Stability of a Residual Soil Slope. *Computers and Geotechnics*, Vol. 26, 2000, pp. 145-165.
- [17] Jakob, M., & Lambert, S. Climate Change Effects on Landslides Along the Southwest Coast of British Columbia. *Geomorphology*, Vol. 107, 2009, pp. 275-284.
- [18] Jotisankasa, A., & Mairaing, W. Suction-Monitored Direct Shear Testing of Residual Soils from Landslide-Prone Areas. *Journal of Geotechnical and Geoenvironmental Engineering*, Vol. 136, No. 3, 2010, pp. 533-537
- [19] Kanjanakul, C., Chubuppakarn, T., & Chalermyanont, T. Rainfall Thresholds for Landslide Early Warning System in Nakhon Si Thammarat. *Arabian Journal of Geoscience*, Vol. 584, 2016.
- [20] Manton, M. J., Della-Marta, P. M., Haylock, M. R., Hennessy, K. J., Nicholls, N., Chambers, L. E., Collins, D. A., Dew, G., Finet, A., Gunawan, D., Inape, K., Isobe, H., Kestin, T. S., Lefale, P., Leyu, C. H., Lwin, T., Maitrepierre, L., Ouprasitwong, N., Page, C. M., Pahalad, L., Plummer, N., Salinger, M. J., Suppiah, R., Tran, V. L., Trewin, B., Tibig, I.,

- & Yee, D. Trends in Extreme Daily Rainfall and Temperature in Southeast Asia and The South Pacific: 1961-1998. *International Journal of Climatology*. Vol. 21, 2001, pp. 269-284.
- [21] Nam, S., Gutierrez, M., Diplas, P., & Petrie, J. Determination of the Shear Strength of Unsaturated Soils Using the Multistage Direct Shear Test. *Engineering Geology*, Vol. 122, 2011, pp. 272-280.
- [22] Rahardjo, H., Li, X. W., Toll, D. G., & Leong, E. C. The Effect of Antecedent Rainfall on Slope Stability. *Geotechnical and Geological Engineering*, Vol. 19, 2001, pp. 371-399.
- [23] Rahardjo, H., Satyanaga, A., & Leong, E. C. Effects of Flux Boundary Conditions on Pore-water Pressure Distribution in Slope. *Engineering Geology*, Vol. 165, 2013, pp. 133-142.
- [24] Soralump, S., Kunsuwan, B., & Torwivat, W. Analysis of Critical API Using for Warning of Heavy Rainfall-induced Landslide. *Proceedings the 12th National Conservation on Civil Engineering, Thailand, 2007.*
- [25] Soralump, S., & Chaithong, T. Modeling Impact of Future Climate on Stability of Slope Based on General Circulation Model. *Geotechnical Engineering Journal of the SEAGS & AGSSEA*, unpublished
- [26] Soralump, S., & Thowiwat, W. Dynamics Landslide Susceptibility Model. *Proceedings the 15th National Convention on Civil Engineering, Thailand, 2010.*
- [27] Thaiyuenwong, S., Nootimthong, B., Datmark, W., & Soralump, S. Landslide Warning by Rainfall Monitoring on Mountainous Area in Northern Thailand. *Proceedings the 18th National Convention on Civil Engineering, Thailand, 2013.*
- [28] Torwivat, W., & Soralump, S. Critical API Model for Landslide Warning. *Proceedings the 14th National Convention on Civil Engineering, Thailand, 2009.*
- [29] Torwivat, W., & Soralump, S. Critical API Model for landslide Warning. *Proceedings the 15th National Convention on Civil Engineering, Thailand, 2010.*

Copyright © Int. J. of GEOMATE. All rights reserved, including the making of copies unless permission is obtained from the copyright proprietors.
